Tunable spin transport in CrAs: Role of correlation effects

L. Chioncel,[1] M. I. Katsnelson,[1] G. A. de Wijs,[1] R. A. de Groot,[1,2] and A. I. Lichtenstein[1,3]
[1]*University of Nijmegen, NL-6525 ED Nijmegen, The Netherlands*
[2]*Materials Science Centre, NL-9747 AG Groningen, The Netherlands*
[3]*Institute of Theoretical Physics, University of Hamburg, Germany*
(Received 13 September 2004; revised manuscript received 18 November 2004; published 10 February 2005)

Correlation effects on the electronic structure of half-metallic CrAs in zinc-blende structure are studied for different substrate lattice constants. Depending on the substrate the spectral weight of the nonquasiparticle states might be tuned from a well-developed value in the case of an InAs substrate to an almost negligible contribution for the GaAs one. A piezoelectric material that would allow a change in the substrate lattice parameters opens the possibility for practical investigations of the switchable (tunable) nonquasiparticle states. Since the latter are important for the tunneling magnetoresistance and related phenomena, it creates new opportunities in spintronics.

DOI: 10.1103/PhysRevB.71.085111 PACS number(s): 72.25.−b, 71.45.Gm, 71.15.Ap, 75.50.Cc

I. INTRODUCTION

One of the strongest motivations to investigate magnetic semiconductors and half-metallic ferromagnets (HMF's) is the possibility to design and produce novel stable structures on semiconducting substrates with new interesting properties. Adopting this point of view first-principles studies are an excellent starting point to predict new systems having the desired properties. Recently Akinaga *et al.*[1] found the possibility to fabricate zinc-blende- (ZB-) type CrAs half-metallic ferromagnetic material. Experimental data confirmed that this material is ferromagnetic with a magnetic moment of $3\mu_B$, in agreement with theoretical predictions.[1] According to this calculation this half-metallic material has a gap of about 1.8 eV in the minority-spin channel which has attracted much attention to this potential candidate for spintronic applications, keeping in mind also its high Curie temperature T_c around 400 *K*. Note that recent experiments on CrAs epilayers grown on GaAs(001) evidenced an orthorhombic structure, different from the ZB one, so the structure is rather sensitive to the preparation process.[2] However, it is highly desirable to explore the possibility of the existence of half-metallic ferromagnetism in materials which are compatible with important III-V and II-IV semiconductors. For this purpose effort has been made on the metastable ZB structures, such as CrAs.[1,3] Beyond the importance of the preparation techniques, attention should be given to the understanding of the finite-temperature properties in these HMF materials. Therefore, it is interesting to explore theoretically the mechanism behind half-metallic ferromagnetism at finite temperature from a realistic electronic structure point of view.

Theoretical studies[4] of the 3*d* transition-metal monoarsenides have shown that the ferromagnetic phase of the ZB structure CrAs compound should be more stable than the antiferromagnetic one. The calculated equilibrium lattice constant is larger than that of GaAs (5.65 Å) having a value of 5.80 Å (Ref. 4). Following this work similar electronic structure calculations concerning the stability of the half-metallic ferromagnetic state in the ZB structure have been carried out.[5]

However, standard local density approximation (LDA) [or generalized gradient approximation (GGA), LDA+U, etc.] calculations are in general insufficient to describe some important many-particle features of the half-metallic ferromagnets. One of these many-body features, the nonquasiparticle (NQP) states[6–8] contribute essentially to the tunneling transport in heterostructures containing HMF's.[9,10] The origin of these states is connected with the "spin-polaron" processes: the spin-down low-energy electron excitations, which are forbidden for HMF's in the one-particle picture, turn out to be possible as superpositions of spin-up electron excitations and virtual magnons.[6,7] Recently we have applied the LDA+DMFT (dynamical mean-field theory) approach[11,13] to describe from first principles the nonquasiparticle states in a prototype half-metallic ferromagnet NiMnSb.[14]

In this paper, we describe the correlation effects in CrAs HMF material in the framework of the LDA+DMFT approach. We will show that these many-body spin-polaron processes are very sensitive to structural properties of the artificially produced CrAs compound. Depending on the substrate characteristics, such as a large lattice constant, as in the case of InAs (6.06 Å), or a smaller one, as in the case of GaAs (5.65 Å), the spectral weight of the nonquasiparticle states can be tuned from a large value in the former case (InAs) to an almost negligible contribution in the later case (GaAs). Therefore, the correlation effects in conjunction with structural properties determine the behavior of electronic states in CrAs near the Fermi level which has a substantial impact on the tunneling transport in the corresponding heterostructures.

II. TUNNELING TRANSPORT AND NONQUASIPARTICLE PHYSICS

First, let us explain in a simple way why the nonquasiparticle states are important for the tunneling transport (for formal derivations, see Refs. 9 and 10). To this aim we consider the case of a narrow-band saturated Hubbard ferromagnet where the current carriers are the holes in the lowest Hubbard band and the nonquasiparticle states provide *all* spectral

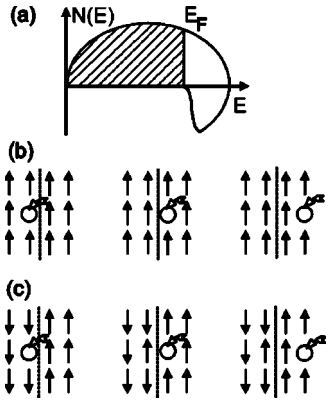

FIG. 1. The tunneling transport between strongly correlated ferromagnets. The density of states in the lower Hubbard band (a) is provided by standard current states for majority-spin electrons (above) and by nonquasiparticle states for minority-spin electrons (below), the latter contribution being nonzero only above the Fermi energy (occupied states are shadowed). However, tunneling is possible both for parallel (b) and antiparallel (c) magnetization directions.

weight for the minority-spin projection.[7] A schematic density of states is shown in Fig. 1(a). Suppose we have a tunnel junction with two pieces of this ferromagnet with either parallel [Fig. 1(b)] or antiparallel [Fig. 1(c)] magnetization directions. From the one-particle point of view, spin-conserving tunneling is forbidden in the latter case. However, in the framework of the many-particle picture the charge current is a transfer process between an empty site and a single-occupied site rather than the motion of the electron irrespective to the site like in the band theory, and therefore the distinction between these two cases (see Fig. 1) is due only to the difference in the densities of states. It means that the estimations of the tunneling magnetoresistance based on a simple one-electron picture is too optimistic; even for antiparallel spin orientation of two pieces of the half-metallic ferromagnets in the junction for zero temperature, the current is not zero, due to the nonquasiparticle states. More exactly, it vanishes for zero bias since the density of NQP states at the Fermi energy equals to zero. However, it grows with bias sharply, having the scale of order of typical *magnon* energies—that is, millivolts.

The latter statement is confirmed by a formal consideration of the antiparallel spin orientation case, based on the standard tunneling Hamiltonian[15]

$$H = H_L + H_R + \sum_{kp} (T_{kp} c^{\dagger}_{k\uparrow} c_{p\downarrow} + \text{H.c.}), \tag{1}$$

where $H_{L,R}$ are the Hamiltonians of the left (right) half-spaces, k and p are corresponding quasimomenta, and spin projections are defined with respect to the magnetization direction of a given half-space with opposite magnetization directions (spin is supposed to be conserving in the "global" coordinate system). For the tunneling current I in the second order in T_{kp} one has

$$I \propto \sum_{kqp} |T_{kp}|^2 [1 + N_q - f(t_{p-q})] \times [f(t_k) - f(t_k + eV)] \delta(eV + t_k - t_{p-q} + \omega_q), \tag{2}$$

where e is the electron charge and V is the bias.[9] The differential conductance of the junction with antiparallel magnetization directions is just proportional (for zero temperature) to the density of nonquasiparticle states:

$$dI/dV \propto N_{NQP}(eV).$$

Note that the value $N_{NQP}(eV)$ vanishes for $|eV| < \hbar\omega_0$, where $\hbar\omega_0$ is an anisotropy gap in the magnon spectrum,[9] which is small, but could be changed by suitable substitution.[16] It is worthwhile to note also that the nonquasiparticle states play an important role (together with the classical effect of the smearing of the gap by spin-disorder scattering) in the depolarization of the states near the Fermi energy at finite temperatures; again, estimations of the tunneling magnetoresistance based on a simple Stoner-like picture of the energy spectrum appear to be completely unrealistic.[17]

III. NONQUASIPARTICLE STATES AND ELECTRONIC STRUCTURE

To perform the calculations we used the newly developed LDA+DMFT scheme.[18] This method is based on the so-called exact muffin-tin orbitals (EMTO) scheme[19,20] within a screened Korringa-Kohn-Rostoker (KKR)[21] approach, frozen core together with the LDA. The correlation effects are treated in the framework of DMFT,[22] with a spin-polarized T-matrix fluctuation exchange (SPTF) type of DMFT solver.[23] The SPTF approximation is a multiband spin-polarized generalization of the fluctuation exchange approximation (FLEX),[12,13] but with a different treatment of particle-hole (PH) and particle-particle (PP) channels. The PP channel is described by a T-matrix approach[24] giving a renormalization of the effective interaction. This effective interaction is used explicitly in the particle-hole channel. Justifications, further developments, and details of this scheme can be found in Ref. 23. The spin-polaron process is described by the fluctuation potential matrix $W^{\sigma\sigma'}(i\omega)$ with $\sigma = \pm$, defined in a similar way as in the spin-polarized FLEX approximation:[13]

$$\hat{W}(i\omega) = \begin{pmatrix} W^{++}(i\omega) & W^{+-}(i\omega) \\ W^{-+}(i\omega) & W^{--}(i\omega) \end{pmatrix}. \tag{3}$$

The essential feature here is that the potential (3) is a complex energy-dependent matrix in spin space with *off-diagonal* elements:

$$W^{\sigma,-\sigma}(i\omega) = U^m [\chi^{\sigma,-\sigma}(i\omega) - \chi_0^{\sigma,-\sigma}(i\omega)] U^m, \tag{4}$$

where U^m represents the bare vertex matrix corresponding to the transverse magnetic channel, $\chi^{\sigma,-\sigma}(i\omega)$ is an effective transverse susceptibility matrix, and $\chi_0^{\sigma,-\sigma}(i\omega)$ is the bare transverse susceptibility.[13] $i\omega$ are fermionic Matsubara frequencies and (m) corresponds to the magnetic interaction

channel.[12,13] The local Green functions as well as the electronic self-energies are spin diagonal for collinear magnetic configurations. In this approximation the electronic self-energy is calculated in terms of the effective interactions in various channels. The particle-particle contribution to the self-energy was combined with the Hartree-Fock and second-order contributions.[13] To ensure a physical transparent description in the current implementation the combined particle-particle self-energy is presented by its a Hartree $\Sigma^{(TH)}$ and Fock $\Sigma^{(TF)}$ types of contributions:

$$\Sigma = \Sigma^{(TH)} + \Sigma^{(TF)} + \Sigma^{(ph)}, \tag{5}$$

where the particle-hole contribution $\Sigma^{(ph)}$ reads

$$\Sigma^{(ph)}_{12\sigma} = \sum_{34\sigma'} W^{\sigma\sigma'}_{1342} G^{\sigma'}_{34}. \tag{6}$$

Since some part of the correlation effects are included already in the local spin density approximation (LSDA) "double counted" terms should be taken into account. To this aim, we start with the LSDA electronic structure and replace $\Sigma_\sigma(E)$ by $\Sigma_\sigma(E)-\Sigma_\sigma(0)$ in all equations of the LDA+DMFT method,[25] the energy E being relative to the Fermi energy and $E_F=0$. It means that we only add *dynamical* correlation effects to the LSDA method.

In our calculations we considered the standard representation of the zinc-blende structure with an fcc unit cell containing four atoms: Cr(0,0,0), As(1/4,1/4,1/4), and two vacant sites $E(1/2,1/2,1/2)$ and $E1(3/4,3/4,3/4)$. We used the experimental lattice constant of GaAs(5.65 Å) and InAs(6.06 Å) for all the calculations, and the equilibrium value for the bulk CrAs(a_{eq}=5.8 Å), obtained by full-potential linear augmented plane-wave (FLAPW) calculations.[4] To calculate the charge density we integrate along a contour on the complex energy plane which extends from the bottom of the band up to the Fermi level,[20] using 30 energy points. For the Brillouin zone integration we sum up a k-space grid of 89 points in the irreducible part of the Brillouin zone. A cutoff of $l_{\max}=8$ for the multipole expansion of the charge density and a cutoff of $l_{\max}=3$ for the wave functions were used. The Perdew-Wang[26] parametrization of the LDA to the exchange correlation potential was used.

IV. RESULTS AND DISCUSSIONS

The LDA+DMFT calculations were carried out for three lattice constants: the GaAs, InAs, and the "equilibrium" one. The corresponding LDA computational results agree with previous ones.[1,4,27] In order to evaluate the average Coulomb interaction on the Cr atoms and the corresponding exchange interactions we start with the constrained LDA method.[28] In our case the constrained LDA calculation indicates that the average Coulomb interaction between the Cr 3d electrons is about U=6.5 eV with an exchange interaction energy about J=0.9 eV. It is important to note that the values of the average Coulomb interaction parameter slightly decrease going from the GaAs(U=6.59 eV) to InAs(U=6.25 eV) lattice constants; see Table I. This is in agreement with a naive picture of a less effective screening due to increasing of the distances between the atoms.

TABLE I. The muffin-tin radii of the Cr, As, and the two types of empty spheres placed as vacancies of the ZB structure. The constreined LDA values for the Coulomb and exchange interactions are presented.

	Cr (a.u.)	As (a.u.)	E (a.u.)	$E1$ (a.u.)	U (eV)	J (eV)
R_{MT}^{GaAs}	2.565	2.688	2.565	2.688	6.59	0.93
$R_{MT}^{eq.}$	2.633	2.759	2.633	2.759	6.46	0.93
R_{MT}^{InAs}	2.751	2.883	2.751	2.883	6.25	0.93

The typical insulating screening used in the constraint calculation[28] should be replaced by a metallic kind of screening. The metallic screening will lead to a smaller value of U. Unfortunately, there are no reliable schemes to calculate U in metals; therefore, we choose some intermediate value of U =2 eV and J=0.9 eV. It is important to realize that there are no significant changes in the values of the average Coulomb interaction for the studied lattice structures and that the exchange interaction is practically constant. Note that physical results are not very sensitive to the value of U, as was demonstrated by us for NiMnSb.[14]

The LSDA and LSDA+DMFT calculations for the density of states (DOS) are presented in Fig. 2. Depending on the lattice constant the Cr and As atoms lose electrons and this charge is gained by the vacant sites. As a result the Fermi level is moving from the right edge of the gap as for the case of GaAs substrate, towards the middle of the gap for a InAs substrate. The Cr moments are well localized due to a mechanism similar to that of localization of the magnetic moment on the Mn atom in the Heusler NiMnSb.[29] Note that

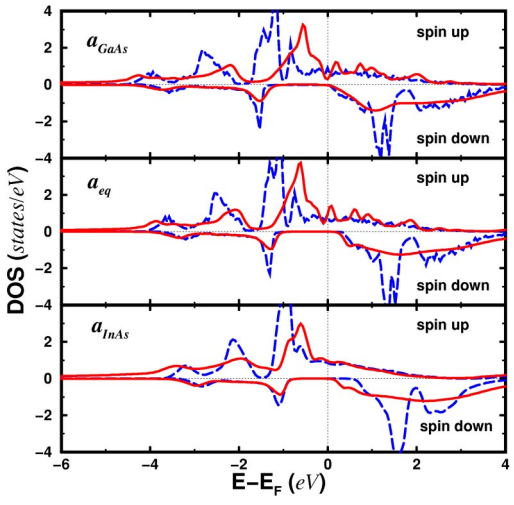

FIG. 2. Cr density of states calculated in the LSDA (dashed line) and LSDA+DMFT (solid line) methods corresponding to a temperature of T=200 K, average Coulomb interaction parameter U =2 eV, and exchange J=0.9 eV. The nonquasiparticle states are clearly visible for lattice parameters larger than a_{eq}=5.8 Å, in the unoccupied part for the minority-spin channel just above the Fermi level, around 0.5 eV.

TABLE II. Summarizing table containing the results of our calculation. CrAs magnetic moments corresponding to the GaAs, InAs, and the equlibrium lattice constant a_{eq}. For the latter one the value a_{eq} =5.8 Å was used (Ref. 4). Parameters of the DMFT calculations are presented in the last three columns of the table.

	Cr (μ_B)	As (μ_B)	E (μ_B)	$E1$ (μ_B)	Total (μ_B)	T (K)	U (eV)	J (eV)
μ_{LDA}^{GaAs}	3.191	−0.270	−0.009	0.089	3.00	—	—	—
μ_{DMFT}^{GaAs}	3.224	−0.267	−0.023	0.067	3.00	200	2	0.9
$\mu_{LDA}^{eq.}$	3.284	−0.341	−0.018	0.076	3.00	—	—	—
$\mu_{DMFT}^{eq.}$	3.290	−0.327	−0.024	0.068	3.00	200	2	0.9
μ_{LDA}^{InAs}	3.376	−0.416	−0.025	0.066	3.00	—	—	—
μ_{DMFT}^{InAs}	3.430	−0.433	−0.033	0.043	3.00	200	2	0.9

the local Cr spin moment is more than $3\mu_B$ and the As atom possesses a small induced magnetic moment (of order of $-0.3\mu_B$) coupled antiparallel to the Cr one. The results are presented in Table II. Calculated, DMFT, and Cr magnetic moments increased in comparison with the LDA results, due to the localization tendency of the Cr $-3d$ states as a consequence of correlation effects.[18]

According to our calculations, the system remains half-metallic with a fairly large band gap (about 1.8 eV) for all lattice constants compared with the band gap of the NiMnSb which is only 0.75 eV.[29]

In Fig. 2 the nonquasiparticle states are visible for lattice parameter higher than the equilibrium one, with a considerable spectral weight in the case of the InAs substrate. InAs is widely used as substrate material for the growth of different compounds. According to our calculations this situation is very favorable for the experimental investigation of the formation of nonquasiparticle states as well as the investigation of their nature.

Comparing with the case of the GaAs lattice parameter, for the InAs substrate, the most significant change in the electronic structure is suffered by the As p states. Having a larger lattice constant the Cr atom acquires a slightly larger magnetic moment. In the LDA calculations, nevertheless, the magnetic moment per unit cell is integer $3\mu_B$. Expanding the lattice constant from the GaAs to the InAs lattice the Cr states become more atomic like and therefore the spin magnetic moment increases. This is reflected equally in the charge transfer which is smaller for the InAs lattice parameters. A larger Cr moment induces a large spin polarization of the As p states, compensating the smaller p-d hybridization, the total moment remaining at its integer value of $3\mu_B$ (Ref. 27.

Note that the essential difference of the many-body electronic structure for the lattice constants of GaAs and InAs is completely due to the difference in the position of the Fermi energy with respect to the minority-spin band gap whereas the self-energy characterizing the correlation effects is not changed too much (Fig. 3). The total density of states $N(E)$ is rather sensitive to the difference between the band edge E_c and the Fermi energy E_F. If this difference is very small (i.e., the system is close to the electronic topological transition $E_c \rightarrow E_F$), one can use a simple expression for the singular contribution to the bare density of states, $\delta N_0(E) \propto \sqrt{E-E_c}(E>E_c)$. The appearance of the complex self-energy $\Sigma(E)=\Sigma_1(E)-i\Sigma_2(E)$ changes the singular contribution as

$$\delta N(E) \propto [\sqrt{Z_1^2(E)+\Sigma_2^2(E)}+Z_1(E)]^{1/2}, \tag{7}$$

where $Z_1(E)=E-E_c-\Sigma_1(E)$ (cf. Ref. 30). Assuming that the self-energy is small in comparison with $E-E_c$ one can find for the states in the gap $\delta N(E) \propto \Sigma_2(E)/\sqrt{E_c-E}(E<E_c)$. One can see that the shift of the gap edge changes drastically the density of states for the same $\Sigma_2(E)$.

In the remaining part of the paper we elaborate more on the possibility of the practical use of tunable properties of nonquasiparticle states in CrAs grown on different substrates. For most of the applications room temperature and the stability of the ferromagnetic state are the most important prerequisites. The ferromagnetic CrAs material might be grown on III-V semiconductors similarly to the zinc-blende CrSb.[33] We observed the presence of the NQP states for CrAs lattice parameters larger than 5.8 Å. It was found experimentally that at 300 K, around this value of the lattice parameter a stable solid solution of $Ga_{0.65}In_{0.35}As$ is

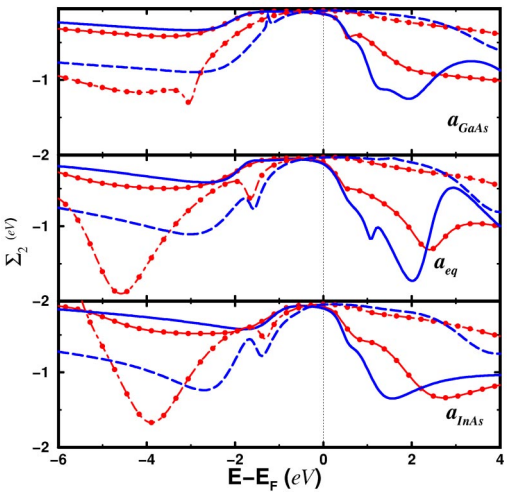

FIG. 3. Energy dependences of imaginary parts of the electron self-energy $\Sigma_2(E)$, for lattice constants of GaAs (a), equilibrium one (b), and InAs (c): e_g, down solid line; t_{2g}, down decorated solid line; e_g, up dashed line; t_{2g}, up decorated dashed line.

formed.[31] So from the practical point of view 65% of gallium in a $Ga_xIn_{1-x}As$ compound would constitute the ideal substrate on which the CrAs half-metal would present tunable properties of its NQP's. Having the $Ga_{0.65}In_{0.35}As$ substrate CrAs could be a part of the epitaxial III-V structure, providing an easy way to integrate with the existing semiconductor technology.

In addition, to determine possible substrates for the growth of layered half-metallic materials, electronic structure calculations were carried out for lattice parameters in the range 5.60–6.03 Å (Ref. 32). According to these calculations,[32] growth with minimal strain might be accomplished in a half-metallic multilayer system grown on InAs substrate which would be the best choice to evidence the NQP states, since the Fermi energy is situated in this case far enough from the bottom of the conduction band.

The existence of NQP states is a manifestation of the many-body interaction at finite temperatures, magnetoelectronic applications being able to measure their presence.

A very high sensitivity of the minority-electron density of states near the Fermi energy to the lattice constant opens a new interesting opportunity to run the current in CrAs-based tunnel junctions. Suppose we have an antiparallel orientation of the magnetizations in the tunnel junction [such as shown in Fig. 1(c)], then the *I-V* characteristic is determined by the density of the nonquasiparticle states. Thus, if we will influence the lattice constant (e.g., using a piezoelectric material), one can modify the differential conductivity. This makes CrAs a very promising material with tunable characteristics which opens new ways for applications in spintronics.

ACKNOWLEDGMENTS

This work is part of the research programme of the Stichting voor Fundamenteel Onderzoek der Materie (FOM), which is financially supported by the Nederlandse Organisatie voor Wetenschappelijk Onderzoek (NWO).

[1] H. Akinaga, T. Magano, and M. Shirai, Jpn. J. Appl. Phys., Part 2 **39**, L1118 (2000).
[2] V. H. Etgens, P. C. de Camargo, M. Eddrief, R. Mattana, J. M. George, and Y. Garreau, Phys. Rev. Lett. **92**, 167205 (2004).
[3] M. Mizguchi, H. Akinaga, T. Manago, K. Ono, M. Oshima, M. Shirai, M. Yuri, H. J. Lin, H. H. Hsieh, and C. T. Chen, J. Appl. Phys. **91**, 7917 (2002).
[4] M. Shirai, Physica E (Amsterdam) **10**, 143 (2001); J. Appl. Phys. **93**, 6844 (2003).
[5] W. H. Xie, Y. Q. Xu, B. G. Liu, and D. G. Pettifor, Phys. Rev. Lett. **91**, 037204 (2003).
[6] D. M. Edwards and J. A. Hertz, J. Phys. F: Met. Phys. **3**, 2191 (1973).
[7] V. Yu. Irkhin and M. I. Katsnelson, Fiz. Tverd. Tela (Leningrad) **25**, 3383 (1983) [Sov. Phys. Solid State **25**, 1947 (1983)]; J. Phys.: Condens. Matter **2**, 7151 (1990).
[8] V. Yu. Irkhin and M. I. Katsnelson, Phys. Usp. **37**, 659 (1994).
[9] V. Yu. Irkhin and M. I. Katsnelson, Eur. Phys. J. B **30**, 481 (2002).
[10] E. McCann and V. I. Fal'ko, Phys. Rev. B **68**, 172404 (2003).
[11] V. I. Anisimov, A. I. Poteryaev, M. A. Korotin, A. O. Anokhin, and G. Kotliar, J. Phys.: Condens. Matter **9**, 7359 (1997); A. I. Lichtenstein and M. I. Katsnelson, Phys. Rev. B **57**, 6884 (1998).
[12] N. E. Bickers and D. J. Scalapino, Ann. Phys. (N.Y.) **193**, 206 (1989).
[13] M. I. Katsnelson and A. I. Lichtenstein, J. Phys.: Condens. Matter **11**, 1037 (1999).
[14] L. Chioncel, M. I. Katsnelson, R. A. de Groot, and A. I. Lichtenstein, Phys. Rev. B **68**, 144425 (2003).
[15] G. D. Mahan, *Many-Particle Physics* (Plenum Press, New York, 1990), Sec. 9.3.
[16] J. J. Attema, C. M. Fang, L. Chioncel, G. A. de Wijs, A. I. Lichtenstein, and R. A. de Groot, J. Phys.: Condens. Matter **16**, S5517 (2004).
[17] V. Yu. Irkhin, M. I. Katsnelson, and A. I. Lichtenstein, cond-mat/0406487 (unpublished).
[18] L. Chioncel, L. Vitos, I. A. Abrikosov, J. Kollár, M. I. Katsnelson, and A. I. Lichtenstein, Phys. Rev. B **67**, 235106 (2003).
[19] O. K. Andersen and T. Saha-Dasgupta, Phys. Rev. B **62**, R16 219 (2000).
[20] L. Vitos, H. L. Skriver, B. Johansson, and J. Kollár, Comput. Mater. Sci. **18**, 24 (2000); L. Vitos, Phys. Rev. B **64**, 014107 (2001).
[21] P. Weinberger, in *Electron Scattering Theory for Ordered and Disordered Matter* (Clarendon Press, Oxford, 1990).
[22] A. Georges, G. Kotliar, W. Krauth, and M. J. Rozenberg, Rev. Mod. Phys. **68**, 13 (1996).
[23] M. I. Katsnelson and A. I. Lichtenstein, Eur. Phys. J. B **30**, 9 (2002).
[24] V. M. Galitski, Zh. Eksp. Teor. Fiz. **34**, 115 (1958); **34**, 1011 (1958); J. Kanamori, Prog. Theor. Phys. **30**, 275 (1963).
[25] A. I. Lichtenstein, M. I. Katsnelson, and G. Kotliar, Phys. Rev. Lett. **87**, 067205 (2001).
[26] J. P. Perdew and Y. Wang, Phys. Rev. B **45**, 13 244 (1992).
[27] I. Galanakis and P. Mavropoulos, Phys. Rev. B **67**, 104417 (2003).
[28] V. I. Anisimov and O. Gunnarsson, Phys. Rev. B **43**, 7570 (1991).
[29] R. A. de Groot, F. M. Mueller, P. G. van Engen, and K. H. J. Buschow, Phys. Rev. Lett. **50**, 2024 (1983).
[30] M. I. Katsnelson and A. V. Trefilov, Z. Phys. B: Condens. Matter **80**, 63 (1990).
[31] H. B. Harland and J. C. Woolley, Can. J. Phys. **44**, 2715 (1966).
[32] C. Y. Fong, M. C. Qian, J. E. Pask, L. H. Yang, and S. Dag, Appl. Phys. Lett. **84**, 239 (2004).
[33] J. H. Zhao, F. Matsukura, K. Takamura, E. Abe, D. Chiba, and H. Ohno, Appl. Phys. Lett. **79**, 2776 (2001).